第 36 卷第 2 期
2017 年 4 月

红外与毫米波学报
J. Infrared Millim. Waves

Vol. 36, No. 2
April, 2017

文章编号: 1001 - 9014(2017)02 - 0135 - 04

DOI:10.11972/j.issn.1001 - 9014.2017.02.002

Low-defect surfaces of low-temperature GaSb thin films on GaSb substrates

HAO Rui-Ting[1*], REN Yang[1], LIU Si-Jia[1], GUO Jie[1],
WANG Guo-Wei[2,3], XU Ying-Qiang[2,3*], NIU Zhi-Chuan[2,3]

(1. Key Laboratory of Renewable Energy Advanced Materials and Manufacturing Technology Ministry of Education, Institute of Solar Energy, Yunnan Normal University, Provincial Key Laboratory of Rural Energy Engineering, Kunming 650500, China;
2. State Key Laboratory for Superlattices and Microstructures, Institute of Semiconductors, Chinese Academy of Sciences, Beijing 100083, China;
3. Synergetic Innovation Center of Quantum Information and Quantum Physics, University of Science and Technology of China, Hefei 230026, China)

Abstract: The influence on the low-defect surface of GaSb thin-film material by the ratio of Sb to Ga (V/III) along with the reducing of the growth temperature was investigated systematically. In order to obtain a good surface morphology of the GaSb epitaxial layer with low defect, both of the growth temperature and the V/III ratio should be reduced at the same time. The optimal growth conditions of Low-temperature GaSb thin films are that the growth temperature is T_c +60℃ and the V/III ratio is about 7.1 when Sb cracker temperature is 900℃.

Key words: low-defect, GaSb, AFM, V/III
PACS: 81.05 Ea, 81.15 Hi

GaSb 衬底上分子束外延生长的低温 GaSb 薄膜的低缺陷表面

郝瑞亭[1*], 任 洋[1], 刘思佳[1], 郭 杰[1], 王国伟[2,3], 徐应强[2,3*], 牛智川[2,3]

(1. 云南师范大学 太阳能研究所,可再生能源材料先进技术与制备教育部重点实验室,
云南省农村能源工程重点实验室,云南 昆明 650500;
2. 中国科学院半导体研究所 半导体超晶格国家重点实验室,北京 100083;
3. 中国科学技术大学 量子信息与量子科技前沿协同创新中心,安徽 合肥 230026)

摘要:系统地研究了随着 GaSb 薄膜生长温度的降低,Sb/Ga(V/III)比的变化对薄膜低缺陷表面质量的影响.为了获得良好表面形貌的 GaSb 外延层,生长温度与 V/III 比均需要同时降低.当 Sb 源裂解温度为 900℃时,生长得到低缺陷表面的低温 GaSb 薄膜的最佳生长条件是生长温度为在再构温度的基础上加 60℃且 V/III 比为 7.1.

关 键 词:低缺陷;锑化镓;原子力显微镜;V/III 比

中图分类号:TN21　　**文献标识码**:A

Introduction

Infrared detectors with multiband detection capabilities are important for highly demanding applications in target identification, recognition, and tracking in recent years. Multicolor detectors can also be used to determine the absolute temperature of targets, which is very useful in medical diagnostics and astronomy. Dual band detectors have already been realized in commercially available technologies such as mercury-cadmium-telluride[1] detectors and quantum well infrared photodetectors[2]. Both sequential mode and simultaneous mode integrated multicolor MCT focal plane arrays (FPAs) have been real-

Received date: 2016-07-11, **revised date**: 2016-12-13　　**收稿日期**:2016-07-11, **修回日期**:2016-12-13
Foundation items: Supported by National Natural Science Foundation of China (11474248, 61176127, 61006085, 61274013, 61306013), Key Program for International S&T cooperation Projects of China (2011DFA62380), and Ph. D. Programs Foundation of Ministry of Education of China (20105303120002)
Biography: HAO Rui-Ting (1979-), male, Henan, Ph. D., associate professor. Research area involves PV materials and devices.
* **Corresponding author**: E-mail: ruitinghao@semi.ac.cn, yingqxu@semi.ac.cn

ized[3-6].

Sb-based dual-band detectors have been fabricated and characterized[7]. Antimony (Sb) based materials are suitable for the fabrication of optoelectronic devices in the mid-infrared wavelength range. Such detectors are useful for several applications, including atmospheric remote sensing. In such applications, the simultaneous detection of optical signals at different wavelengths allows monitoring several atmospheric species with a single excitation source and receiver[8-10].

Designing our next experimental study programs, a dual-band detector tailored to detect wavelengths in the range of 0.8 to 4 μm will be fabricated and characterized. The first band consists of an InAs/GaSb superlattice (or InAsSb) pin architecture for medium (or short) wavelength detection, and the second band consists of a GaSb pin architecture for shorter wavelength detection. However, the GaSb pin architecture needs to be grown at low temperature, because that the growth temperature of InAs/GaSb superlattice (SL) (or InAsSb alloy) material is generally lower than the growth temperature of GaSb buffer layer. Meanwhile, the introduction of a low-temperature buffer layer can significantly improve the crystal quality of InAsSb or InAs/GaSb SL material of the dual-band detector[11].

In addition, many epitaxial structures of the photovoltaic device include a GaSb cap layer. This GaSb layer need to be grown at low temperature in the growth process, so that the quality of this layer directly or indirectly affects the material quality and the electrical and optical behavior of the photovoltaic device[12]. In this paper, we report on the correlation between the growth temperature of GaSb thin films and the ratio of Sb to Ga for the purpose of low-defect surface of the GaSb material grown at low temperature.

1 Experiment

The samples in this study were grown using a Veeco Gen II molecular-beam epitaxy system equipped with valved cracker sources for group V (Sb_2 and As_2) fluxes and Ga/In SUMO® cells, on n-type epiready GaSb (001) substrates. Pairs of samples were grown under the same nominal conditions. First, a 0.2 ~ 0.4 μm nominally undoped GaSb buffer layer was deposited with the growth temperature at T_c + 110℃. Then, an overall total layer thickness was maintained at 550 nm for the undoped GaSb thin-film layers. The thin-film materials were grown at T_c + 60℃ and T_c + 40℃.

T_c is defined as the crossover temperature at which a GaSb surface reconstruction ($2\times5 \leftrightarrow 1\times3$) at a given antimony stabilization flux, according to a calibrated pyrometer. It was noted that all this work was carried out using cracked Sb sources. The cracker tip temperature and base temperature for Sb cells were 900℃ and 580℃, respectively. The V/III flux ratios were measured using a beam equivalent pressure (BEP) gauge. The group III fluxes used in this study produced a growth rate of approximately 0.5 ML/s for the GaSb. In order to investigate the influence of the Ga and Sb beam flux pressure on the GaSb island size and density, the growth temperatures were fixed.

2 Results and discussions

The surface morphological features of the samples were studied by atomic force microscope (AFM). There is a strong correlation between the surface roughness and the properties of the material, according to the previous literatures[13]. When the growth temperature of GaSb thin films was T_c + 60℃, we have achieved the root mean square surface (RMS) surface roughness of the first series of GaSb epilayer samples over an area of 20 μm × 20 μm (using the scanning probe microscopy data analysis software Gwyddion). The results to be discussed in this work were summarized in Table 1. When the V/III ratio was 7.169, the RMS roughness was 1.907 Å, which was the minimum value of the data obtained in the actual experiments.

Table 1 The RMS roughness of the first series of GaSb thin-film samples over an area of 20 μm × 20 μm

表 1 第一批 GaSb 薄膜样品扫面范围为 20 μm × 20 μm 时的表面粗糙度

	V/III	RMS (20 μm × 20 μm)
T_c + 60℃	8.29	3.004 Å
	7.97	2.355 Å
	7.509	2.392 Å
	7.169	1.907 Å
	6.496	2.086 Å
	5.99	2.821 Å

AFM images show many visible bright spots and islands on the surfaces indicating the poor surface morphology of the first series of GaSb thin films as shown in Figs. 1(a) and (b). AFM measurements made on the GaSb thin films showed an extremely defect structure with the present of the clear pyramid protrusion, ups and downs. Figures 1(c) and (d) show representative low-defect AFM images of as-grown GaSb thin-films surface. By observing the surface morphology of the samples shown in Figs. 1(c) and (d), clear and smooth atomic steps are visible over the 5 μm × 5 μm scan area, indicating excellent surface atomically smoothness and the low-defect surfaces of the GaSb thin films, when the V/III ratio was approximately equal to 7.169.

Comparing the surface quality of these GaSb thin-film samples using the microscope, when the growth temperature is T_c + 60℃ and the Sb cracker temperature is 900℃, there are visible changes presented on the surfaces under the 20 times magnification microscope, as shown in Fig. 2. From Fig. 2(a) to Fig. 2(b), it was found that the islands defects on the surface clearly become less; but from Fig. 2 (b) to Fig. 2 (c), the defects with the visible island structure on the surface become more.

When the growth temperature of the second series of GaSb thin-film samples was T_c + 40℃, we achieved the RMS surface roughness of the GaSb epilayer samples over an area of 20 μm × 20 μm as summarized in Table 2. When the ratio of Sb to Ga is 6.504, the minimum value of RMS roughness obtained in the actual experiments is 1.907 Å.

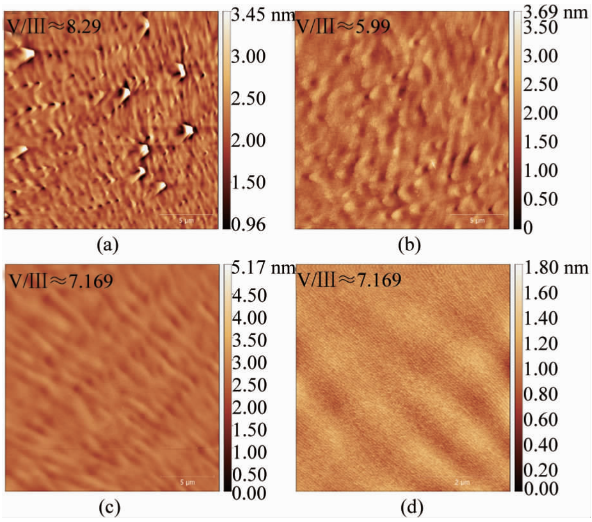

Fig. 1 (a) (b) AFM images of the first series of GaSb thin-film samples surface over 20 μm × 20 μm. (c) (d) AFM images of the first series of GaSb thin-film sample (V/III ≈ 7.169) surface over 20 μm × 20 μm and 5 μm × 5 μm

图 1 (a) (b)第一批 GaSb 薄膜样品 20 μm × 20 μm 的表面形貌 AFM 图,(c) (d)分别为 GaSb 薄膜样品在 V/III 比为 7.169 时 20 μm × 20 μm 和 5 μm × 5 μm 的表面形貌 AFM 图

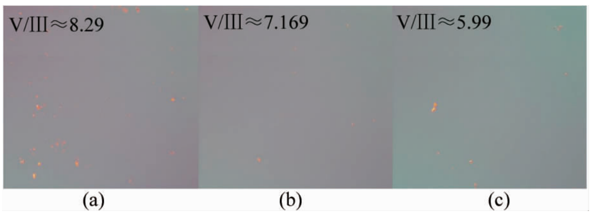

Fig. 2 Microscope images of the samples (T_c + 60 ℃)

图 2 生长温度为 T_c + 60 ℃时样品的显微镜图

Table 2 The RMS roughness of the GaSb thin-film samples over an area of 20 μm × 20 μm

表 2 GaSb 薄膜样品扫面范围为 20 μm × 20 μm 时的表面粗糙度

	V/III	RMS (20 μm × 20 μm)
	7.584	3.781 Å
	7.016	3.554 Å
T_c + 40℃	6.504	2.076 Å
	6.008	2.624 Å
	5.814	2.652 Å
	5.1	3.726 Å

As can be seen from Figs. 3(a) and (b), there are many bright spots on the surfaces of the as-grown samples, namely pyramid structure, indicating that the quality of the surface morphology of the samples is relatively poor. Some of the GaSb thin films prepared in this way show a lot of defects.

When the V/III ratio was approximately equal to 6.504, relatively clear atomic steps are visible over the 5 μm × 5 μm scan area, but the surface quality is still poor and not smooth over the 20 μm × 20 μm scan area, as shown in Figs. 3(c) and (d). Compared with the surface morphology of GaSb thin-film samples under other V/III ratio conditions, there is a relatively low-defect and good quality of surface morphology.

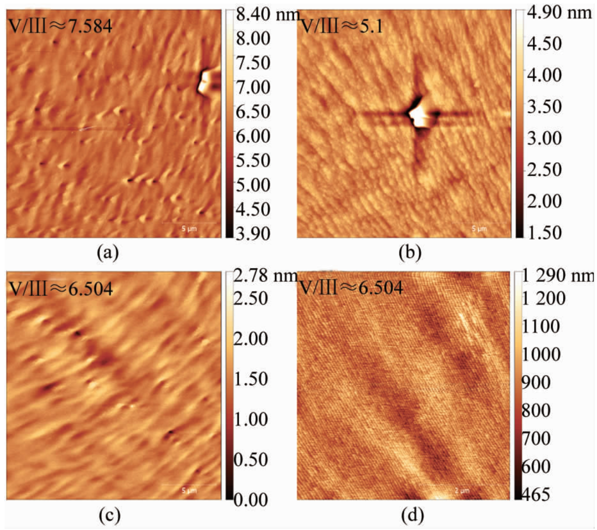

Fig. 3 (a) (b) AFM images of the second series of GaSb thin-film samples surface over 20 μm × 20 μm. (c) (d) AFM images of the second series of GaSb thin-film sample (V/III ≈ 6.504) surface over 20 μm × 20 μm and 5 μm × 5 μm

图 3 (a) (b)第二批 GaSb 薄膜样品 20 μm × 20 μm 的表面形貌 AFM 图,(c) (d)分别为 GaSb 薄膜样品在 V/III 比为 6.504 时 20 μm × 20 μm 和 5 μm × 5 μm 的表面形貌 AFM 图

It is shown in Fig. 4 that there is a visible changing regularity of the bright spots defects as presented on the surfaces under the 5 times magnification microscope, similarly to the phenomenon as shown in Fig. 2, when the growth temperature of GaSb thin-film samples is T_c + 40 ℃ and the Sb cracker temperature is 900 ℃.

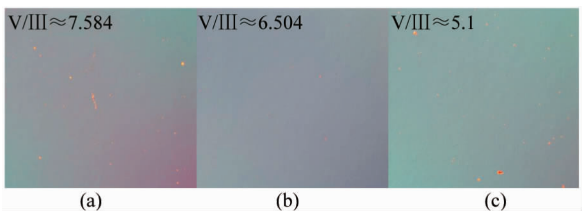

Fig. 4 Microscope images of the samples (T_c + 40 ℃)

图 4 生长温度为 T_c + 40 ℃时样品的显微镜图

When the growth temperature is T_c + 60 ℃ and the V/III ratio is about 7.169, the optimal RMS roughness of the GaSb epilayer sample is around 1.907 Å. However, when the growth temperature is T_c + 40 ℃ and the V/III ratio is about 6.504, the optimal RMS roughness of the GaSb epilayer sample is around 2.076 Å, obtained from the analysis of the surface morphology of the samples in this paper. Compared with Fig. 3, it was clearly observed that the low-defect surface morphology of the sample had a better quality, and the atomic steps are relatively clear and smooth over the 5 μm×5 μm scan area, as shown in Fig. 1.

According to the GaSb thin-film samples data obtained from the different experiments, the fitting curves of the relationship between the RMS roughness and the ratio of Sb to Ga show that when an optimal RMS roughness value obtained from the fitting curve is around 1.987 Å, the V/III ratio is approximately equal to 7.07, and meanwhile, when an optimal RMS roughness value is around 2.49 Å, the V/III ratio is approximately equal to 6.27, when the growth temperature of GaSb epilayer are T_c +60℃ (Fig. 5(a)) and T_c +40℃ (Fig. 5(b)), respectively.

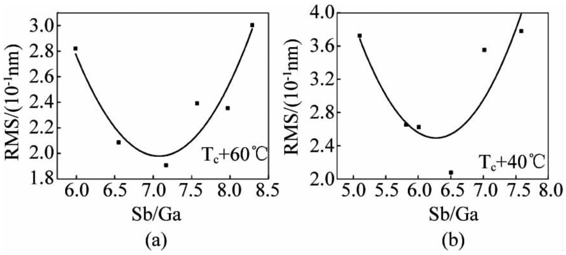

Fig. 5 RMS vs. Sb/Ga. (a) T_c +60℃, (b) T_c +40℃
图5 表面粗糙度与Sb/Ga比关系的拟合曲线:(a)生长温度为 T_c +60℃,(b) 生长温度为 T_c +40℃

According to the relevant literature, with decreasing growth temperature with other parameters remain unchanged, GaSb epitaxial layer surface fully tends to grow island. The island structure density is also increasing, and there are a lot of background defects in the GaSb epitaxial layer[14-16]. Analyzing the fitting curve of RMS vs. Sb/Ga, as shown in Fig. 5, we suspect that the ratio of Sb to Ga should be also reduced with the decreasing growth temperature, so as to get the best quality of the low-defect surface morphology of GaSb thin films grown at low temperature.

3 Conclusion

In this letter, the influences of the growth temperature of GaSb thin film and the ratio of Sb to Ga on the surface morphology are studied. When the growth temperature is reduced, the ratio of Sb to Ga should be also reduced, so as to obtain the GaSb thin films with low defect surface grown at low temperature. Furthermore, T_c +60℃ is the optimal growth temperature for the growth of low-temperature GaSb thin films, when the cracker tip temperature and base temperature for Sb cells are 900℃ and 580℃, respectively. The experimental results obtained in this paper are useful for studying the growth of dual-band detector and the fabrication of low-temperature GaSb based photodetector.

Acknowledgements

This work was supported by National Natural Science Foundation of China (No. 11474248, 61176127, 61006085, 61274013, 61306013), Key Program for International S&T cooperation Projects of China (No. 2011DFA62380), and Ph. D. Programs Foundation of Ministry of Education of China (No. 20105303120002).

References

[1] Cabanski W, Breiter R, Koch R, *et al*. Third gen focal plane array IR detection modules at AIM [J]. *Infrared physics & technology*, 2002, **43**(3):257-263.

[2] Schneider H, Maier T, Fleissner J, et al. Dual-band QWIP focal plane array for the second and third atmospheric windows [J]. *Infrared physics & technology*, 2005, **47**(1): 53-58.

[3] Rogalski A. Recent progress in infrared detector technologies [J]. *Infrared Physics & Technology*, 2011, **54**(3):136-154.

[4] Gautam N, Naydenkov M, Myers S, *et al*. Three color infrared detector using InAs/GaSb superlattices with unipolar barriers [J]. *Applied Physics Letters*, 2011, **98**(12):121106.

[5] Khoshakhlagh A, Rodriguez J B, Plis E, *et al*. Bias dependent dual band response from InAs/Ga(In) Sb type II strain layer superlattice detectors [J]. *Applied Physics Letters*, 2007, **91**(26):263504.

[6] Plis E, Naydenkov M, Myers S, *et al*. Dual-band pBp detectors based on InAs/GaSb strained layer superlattices [J]. *Infrared Physics & Technology*, 2013, **59**:28-31.

[7] Refaat T F, Abedin M N, Bhat I B, *et al*. Sb-based two-color photodetector fabrication and characterization [J]. *Optical Engineering*, 2005, **44**(12):120501.

[8] Abedin M N, Refaat T F, Bhat I B, *et al*. Bias selective operation of Sb-based two-color photodetectors [C]. *SPIE Optics + Photonics. International Society for Optics and Photonics*, 2006: 629709-629709-9.

[9] Rehm R, Walther M, Schmitz J, *et al*. Dual-colour thermal imaging with InAs/GaSb superlattices in mid-wavelength infrared spectral range [J]. *Electronics Letters*, 2006, **42**(10):1.

[10] Abedin M N, Refaat T F, Bhat I B, *et al*. Progress of multicolor single detector to detector array development for remote sensing [C]. *Optical Science and Technology, the SPIE 49th Annual Meeting. International Society for Optics and Photonics*, 2004: 239-247.

[11] Chiu T H, Tsang W T, Ditzenberger J A, *et al*. Growth of InAsSb alloy and InAsSb/GaSb superlattice lattice matched to (100) GaSb by molecular-beam epitaxy [J]. *Journal of applied physics*, 1986, **60**(1):205-207.

[12] Eyink K G, Seaford M L, Haas T W, *et al*. Characterization of low-temperature grown AlSb and GaSb buffer layers [J]. *Journal of Vacuum Science & Technology B*, 1997, **15**(4):1187-1190.

[13] Nguyen B M, Chen G, Hoang M A, *et al*. Growth and characterization of long wavelength infrared type II superlattice photodiodes on a 3 GaSb wafer [C]. *SPIE OPTO. International Society for Optics and Photonics*, 2011: 79451O-79451O-9.

[14] Wang T, Forchel A. Growth of self-organized GaSb islands on a GaAs surface by molecular beam epitaxy [J]. *Journal of applied physics*, 1999, 85(5): 2591-2594.

[15] Ivanov S V, Altukhov P D, Argunova T S, *et al*. Molecular beam epitaxy growth and characterization of thin (<2 mu m) GaSb layers on GaAs (100) substrates [J]. *Semiconductor science and technology*, 1993, **8**(3): 347.

[16] Wu M C, Chen C C. Photoluminescence of liquid - phase epitaxial Te-doped GaSb [J]. *Journal of applied physics*, 1993, **73**(12): 8495-8501.

[17] Iyer S, Small L, Hegde S M, *et al*. Low - temperature photoluminescence of Te-doped GaSb grown by liquid phase electroepitaxy [J]. *Journal of applied physics*, 1995, **77**(11):5902-5909.

[18] Machida R, Toda R, Fujikawa S, *et al*. Effect of low - temperature-grown GaSb layer on formation of high-density and small GaSb islands on Si (100) substrate[J]. *physica status solidi (b)*, 2016.